Journal of Computer Science

Original Research Paper

Radial Basis Function Networks and Contrast-Limited Adaptive Histogram Equalization Filter Based Early-Stage Breast Cancer Detection Techniques

Anitha Ponraj and Aroul Canessane

Department of Computational Science and Engineering, Research Scholar, Sathyabama Institute of Science and Technology, Chennai, India

Article history
Received: 16-02-2023
Revised: 05-05-2023
Accepted: 06-05-2023

Corresponding Author:
Anitha Ponraj
Department of Computational Science and Engineering, Research Scholar, Sathyabama Institute of Science and Technology, Chennai, India
Email: anisainotech@gmail.com

Abstract: Breast cancer is one of the most common types of cancer that kills women. When cells become uncontrollably large, cancer develops. As a result, detecting and classifying breast cancer in its early stages is essential so that patients can take the appropriate precautions. On the other hand, mammography images have relatively low sensitivity and effectiveness in detecting breast cancer. Furthermore, MRI (Magnetic Resonance Imaging) has higher detection sensitivity for breast cancer than mammography. In this research, a novel Radial Basis Function Networks model (RBFN) with a Mayfly Optimization Algorithm (MAO) mechanism has Breast MRI scans aid in the early detection of breast cancer. Following the system's training on Magnetic Resonance Imaging (MRI) breast images, a unique Contrast-Limited Adaptive Histogram Equalization (CLAHE) filter is developed for pre-processing noisy MRI image material. Backgrounds were removed before recovering breast cancer photos with a Contrast Limited Histogram Equalization (CLAHE) filter. Furthermore, the new study effort's performance is compared to earlier studies and this model is simulated using Python. The proposed model, RBFN-MAO, also outperforms previous models in terms of performance and precision with an accuracy of 97.54%. In comparison, it is 85.28, 80.95, 76.94, 85.39 and 90.32% for Convolution Neural Networks You Only Look Once (CNN-YOLO), Residual Networks (ResNet50), Diffusion Convolution Neural Networks (DCNN), Support Vector Machine (SVM) and Convolution Neural Network (CNN) models, respectively.

Keywords: Breast Cancer Prediction, Contrast Limited Histogram Equalization, Mayfly Optimization Algorithm, Computer-Aided Diagnosis, Neural Network, Deep Learning

Introduction

The American Cancer Society and the International Agency for Cancer Research (IARC), two research organizations affiliated with the WHO, claim that cancer incidence has increased globally. World Health Organization (WHO) predicts that by 2040, 27.5 million people will have been diagnosed with cancer, with 16.3 million dying from the disease (Sung *et al*., 2021). Among the leading causes of death for women in industrialized nations, breast cancer is second only to lung cancer (Siegel *et al*., 2020). In developing countries, breast cancer is the second most common type. Common causes of breast cancer include a lack of milk production due to faulty milk ducts (invasive ducal carcinoma). Breast cancer, on the other hand, can develop in other lobules, or tissues, within the breast which are lobules and glandular tissues (Svensson *et al*., 2020).

Approximately 50% of older mammograms developed lesions due to further follow-ups and screenings throughout the diagnostic interval (Duffy *et al*., 2020; Houssami *et al*., 2017; Woodard *et al*., 2007; Warren Burhenne *et al*., 2000). Radiologists questioned if benign previous mammograms without lesion indications would include concealed information indicating a future risk of cancer emergence (Brennan *et al*., 2018).

With one in every eight deaths, breast cancer is the leading cause of death in the globe 6 million deaths per year. Breast cancer will kill more than 20 million women worldwide by 2050. Breast cancer is a prevalent health problem among women. Breast cancer is diagnosed using Magnetic Resonance Imaging (MRI) and mammograms. Radiologists utilize computers to classify abnormalities discovered in mammograms.

The first line of defense against breast cancer is mammography. Mammograms use breast X-rays to detect abnormalities. Mammograms use X-rays to detect breast cancer. This tumor is malignant, benign, and expected all at the same time. Malignant cells are not visible on regular mammography; malignant cells are seen on benign mammograms but not on those of ill women. Each of these three elements must be identified. Mammograms can be analyzed using a variety of approaches (Gaikwad, 2015).

This article discusses recent advances in Breast cancer detection with Machine Learning (ML) and Deep Learning (DL). The purpose of this study was to inform the reader about recent advances in Multiviewdigital mammography and breast cancer research (DMs). The education uses Multiviewdigital mammography data to determine the difficulty of applying deep learning to early breast cancer diagnosis. This study presents a novel RBFN model using a Mayfly Optimization Algorithm (MAO) for the early detection of breast cancer utilizing data from breast MRI. The CLAHE filter was developed to pre-process noisy MRI images after being trained on breast MRI data. The background was removed from breast cancer images before the Contrast Limited Histogram Equalization (CLAHE) filter was applied to finish the task. In addition, a Python simulation of this model is run and the findings are compared to those of the ongoing research effort. The rest of the essay will be structured as surveys: The second unit summarizes the necessary literature on cancer categorization and detection. Outlines the recommended methodology employed in this education. The experimental data for categorizing breast cancer are presented.

Literature Survey

Baffa and Lattari (2018) have static and dynamic versions of various databases. Each of the 42 participants in the study had twenty thermal pictures taken. The experimental design was made up of these three distinct steps. The Convolutional Neural Network (CNN) was trained using both color and grayscale thermography. Compared to dynamic color images, static color, and grayscale shots had 98 and 95% accuracy ratios, respectively, whereas vibrant color images had accuracy ratios of 95 and 92%.

Wang *et al*. (2018) developed a unique Support Vector Machine (SVM) based ensemble learning approach method technique to reduce diagnostic error variance while increasing diagnostic precision. The Support Vector Machine (SVM) based ensemble learning method was also applicable to other illness diagnoses for achieving a safer, more consistent, and more efficient illness diagnosis procedure. Here the relevant feature extraction still needs to be performed.

Guan *et al*. (2018) Utilization of the Diffusion-Convolutional Neural Networks (DCNN) model, which mixes deconvolution and convolutional neural networks. The researchers conducted two studies to classify samples of breast tissue. The first experiment was set to 0.9424 and there were a total of 165 thermal pictures, of which 132 were utilized for training and 33 were used for validation. In the second experiment, then set at 0.8340, 150 thermal images were used for training and ten were utilized for verification. In both studies, both the era and the learning rate were set to 1000.

Charan *et al*. (2018) to correct the issue with a small tumor's size relative to the entire image, the images must first be altered. The maximum classification accuracy that could be achieved was 65%. It's important to remember that the overall accuracy average is the sole statistic considered. F1-score, recall, and precision is not considered.

Huang *et al*. (2017) using large breast cancer datasets, the effectiveness of SVM and SVM ensembles was investigated. SVM ensembles with Radial Basis Function (RBF) kernels and the boosting technique outperformed bagging ensembles of linear kernel-based SVMs on short datasets. As part of the data pre-processing stage, both approaches used feature selection. When working with large datasets and Radial Basis Function (RBF) kernel-based Support Vector Machine (SVM) groups calls for boosting. The accuracy of the projections remained relatively high.

Gbenga *et al*. (2017) Breast cancer in women can now be diagnosed early thanks to computer-aided diagnostic tools. The following are some of the diagnostic applications of mammography: Crushing the breast between two parallel plates is the first stage. As a result, the X-rays can only penetrate a restricted area, resulting in more precise images.

Iqbal *et al*. (2019) to get the desired outcome, the grey level value of each pixel was reduced by 256 after the Database for Mastology Research (DMR) images were converted to grayscale. The following factors were considered before selecting the top five features: 32 features had the Gray Level Co-occurrence Matrix (GLCM) and Run Length Matrix (RLM) applied to them. The results showed that 90.06% of the predictions were correct.

Motlagh *et al*. created a carefully tailored and pre-trained deep neural network (Motlagh *et al*., 2018). Because this was pre-trained using a Residual Neural Network (ResNet) V1 50 model, the generated network has a high degree of specificity in detecting all four types of cancer. More classification of malignant and benign tumor subtypes is possible using ResNet V1 50 and ResNet V1 152. For pathological analysis, however, optimized pre-trained deep neural networks were not appropriate.

Deep Convolutional Neural Networks (DNN) developed by Piantadosi *et al*. (2020) to separate damaged areas in breast pictures automatically. To create an accurate result, the Convolutional Neural Networks (CNN) is also set up in a three-dimensional shape; hence, the outcomes compared to the sickness severity graphs are as follows: It has thus proven useful in obtaining reliable findings across various complex databases. However, the process takes longer to complete than anticipated.

Using three-dimensional Convolutional Neural Networks (CNN) and candidate accretion with a priority function, Tsung-Chen Chiang and colleagues (Chiang *et al*., 2018) created a Computer Aided Detection (CADe) system. To avoid problems caused by over-aggregation, candidates were prioritized during the aggregation process based on the anticipated cancer likelihood. The method fully utilized how the sizes of the Volumes of Interest (VoI) and target tumors relate to one another. However, the rate of breast cancer detection did not significantly improve.

Mambou and colleagues (Mambou *et al*., 2018) Inception V3, a deep convolutional neural network model, was proposed. The Database for Mastology Research (DMR) database contains 1062 thermal pictures, with 80% utilized for training and 20% used for validation. The investigators supplied information regarding the proportion of breast-infected women who were unwell, but the method made no remarks regarding the accuracy rate. Thijs Kooi and colleagues (Kooi *et al*., 2017) described CNNs for mammography reading. The extensive training dataset revealed exceptional sensitivity for Convolutional Neural Networks (CNN). Later, an analysis of the network was performed to certify.

Sadhukhan *et al*. (2020), K-Nearest Neighbour (KNN), Support Vector Machine (SVM) models for early because of a breast cancer diagnosis delaying treatment increases the probability of death. Using the above-mentioned classifier and machine learning perfect following the prediction, the predictive model's effectiveness compared to earlier work is reviewed, resulting in improved outcomes. However, more time will be needed to deploy this technology to detect cancer cells.

Oladipupo *et al*. (2020), proposed an Interval Type-2 fuzzy association rule mining approach for pattern discovery in breast cancer dataset. In the first part of this analysis, the interval Type-2 fuzzification of the breast cancer dataset is carried out using Hao and Mendel approach. In the second part, FP-growth algorithm is adopted for associative pattern discovery from the fuzzified dataset from the first part. To establish the adequacy of the linguistic word defined by the expert, Jaccard similarity measure is used. This analysis is able to discover associative rules with minimum number of symptoms at confidence values as high as 91%.

Zalloum *et al*. (2022), various algorithms of the machine are proposed in designing the classification system for detecting the BC diseases. To improve the resulting quality, the Principal Component Analysis Algorithm (PCA) is applied. The system was tested and evaluated on the Wisconsin BC dataset from the University of Wisconsin Hospitals.

Mohammed *et al*. (2022), proposed the enhanced system of a decision support system based on hybrid classification algorithms to classify breast cancer patients accurately and quickly. The main contribution of this article is to develop an algorithm that filters the data and solves the problem of missing data in some records to facilitate the classification of data. In the experiments conducted, the proposed system was learned by several algorithms on a standard Electronic Health Records (HER) dataset to determine the appropriate test factors.

The recent survey on breast cancer detection was tabulated in Table 1. The gap diagnosed from the above literature survey is detecting the breast cancer of patients with a good rate of prediction and feature extraction from MRI images in early stages that is conquered by the proposed system that combines feature extraction using the mayfly optimization algorithm and CLAHE filter with RBFN network.

Table 1: Recent survey on breast cancer detection

Year	Author	Aim	Methods	Remarks
2021	Sánchez-Cauce *et al*. (2021)	One method for early identification of breast cancer is combining thermal pictures taken from various perspectives with medical and separate information. Convolutional neural networks classify the image analysis multi-input model	of Clinical data is then used to investigate a new branch after thermal pictures are first used to look for structures	Combine front and side images enhance the model's classification performance, and adding clinical and individualized data makes it easier to determine the patient's ailments
2020	Jarosik *et al*. (2020)	Provided a technique for classifying breast size relying on models of the deep learning that use radio frequency and tiny ultrasound data as raw inputs (RF)	Deep-learning models automatically process the amplitude sample data and 2D RF signal patches. RF amplitude data samples parameters are frequently used	The probability that deep learning will be applied to RF data to categorize mass breast development
2021	Chouhan *et al*. (2021)	Introduced the DFeBCD technique, which employs a highway internet-inspired deep convolution neural network to dynamically extract a set of fourth characteristics from mammography (CNN)	The two classifiers, Emotional Learning Ensemble Classifier (ELiEC) and Support Vector Machine, using a typical IRMA dataset of mammogram-trained features (SVM)	The combination of four different features boosts the system's performance by 2-3%. The effectiveness of various classifiers is evaluated using each set of ad hoc features
2020	Xie *et al*. (2020)	Make a multiscale end-to-end deep learning perfect for mammography a classification that can automatically classified with simply class labels and mammogram images	The classifier provides three categories of map features based on categorizing local lesions in conjunction with the global data	Multi-scale techniques can achieve the the same performance when applied to a network with fewer parameters while consuming up to 60% less computing power
2020	Le *et al*. (2020)	Analysis of conventional neural networks is evaluated and created for the integration of Tumour-Infiltrating Lymphocytes (TIL) and cancer maps in standard diagnostic breast cancer full slide tissue images (WSIs)	Three CNN networks-Resnet-34, of VGG16 (Visual Geometry Group), and Inception v4-are used to evaluate TIL and tumor	This open-source application allows the general public to access the TIL/tumor maps for 1.090 TCGA invasive breast cancer pictures

Table 1: Continue

2019	Ellmann *et al*. (2019)	A hybrid Artificial Neural Net-based the method that incorporates functional imaging characteristics are applied to produce macroscopic bone metastases	hybrid PET/CT and MR imaging forecasts is helpful as a non-invasive surrogate markers for early metastatic disease	This method paved the way for the earlier detection of microscopic bone metastases by merging functional and metabolic signs
2020	Kim *et al*. (2020)	A technique for correctly identifying breast cancer on medical images was proposed utilizing side extraction and altered models. Convolutional Recurrent Neural Network (CRNN) the model later to compress images	The efficiency of the procedure is and evaluated using traditional deep learningA modified convolutional recurrent neural network (CRNN) model is used	The accuracy rating for this model is a robust 99.75%, with the lowest loss being 0.0257
2020	Singh *et al*. (2020)	Provided a method to address this problem focused on leveraging the concept of transferring learning to classify histology and imbalanced images	utilizing cutting-edge techniques and a well-known VGG-19 base model on a a sizable dataset with 277,524 images	performing a numerical simulation on a supercomputer for research on transfer learning and unbalanced image classification
2020	George and Sankaran (2020)	This technology has been proven to be a reliable method for automatically diagnosing breast cancer and may be used in a clinical setting	Combine the results of multiple hybrids CNN and SVM-based classifiers	The proposed method achieves superior results to those of cutting-edge techniques without much processing effort
2023	Anitha Ponraj and Arou lCanessane (our research)	The proposed work was conducted to detect the breast cancer of patients with a good rate of prediction and feature extraction from MRI images in early stages that are conquered by the proposed a system that combines Feature Extraction using the Mayfly optimization algorithm a nd CLAHE filter to improve the image quality with RBFN network	The proposed system uses the proposed picture quality improvement technique to distinguish between normal and breast cancer cells. The augmented image is smoothed using a median filter in this manner. A median filter has been proven to reduce impulsive noise, maintain edge information, and not produce any new artificial pixel intensity The proposed segmentation of the mammography pictures are done using the modified U-Net (U-shaped encoder -decoder network architecture) model	The proposed method achieves superior result in those cutting-edge techniques with good prediction in terms of improved accurate in breast cancer prediction

Proposed System

Breast cancer may be difficult to diagnose if a histo-pathological scan displays ad-hoc forms of extremely complex cell structures. The proposed research method is to create an autonomous system for detection and categorization utilizing various machine-learning approaches and several techniques, including histopathology pictures. The framework proposed includes enhancement, nuclei segmentation, feature extraction, and classification.

The block illustration for the projected work is shown in Fig. 1. The input data is pre-processed using the CLAHE method and sent to the segmentation module, where the data is fragmented for further processing. The segmented data is then sent for a feature extraction process using the mayfly optimization algorithm. The data is then classified using the RBFN technique, as shown. Meanwhile, the user can log in for data sensing and uploading on the hospital server that the concerned doctor accesses for future reference and further treatment.

Pre-Processing Using CLAHE Method

Improved comprehension is ensured using image-enhancing techniques. Histogram equalization is one method of increasing the dynamic range of the pixel intensity distribution. Breast cancer image histograms based on contrast which is narrow and focused exclusively on particular grey level values show that which often have shallow contrast. In contrast, the reduced difference in breast cancer pictures obscures the fine details of the lesions, making them challenging to present to specialists. There is a risk of incorrect therapy as a result of this delay. Such situations necessitate histogram equalization, which ignores local variations entirely. Because of the higher background in homogeneities produced by the CLAHE algorithm, some post-processing is necessary for medical imaging. Image quality can be improved by employing a CLAHE-based technique, which is detailed in this article. This is illustrated in Fig. 2 by a succession of non-overlapping "tiles" that the algorithm creates from the image. Listed here are the steps that make up the proposed procedure.

As a starting point, a breast cancer image is selected:

Step I : Select the green layer
Step II : Contextual regions should be divided into two-by-two squares (tiles)
Step III : CLAHE is applied to each tile one by one in step four
Step IV : Apply the median filter to each tile individually in Step V
Step V : Combine four images using the image catenation approach

The augmented image is smoothed using a median filter in this manner. A median filter has been proven to reduce impulsive noise, maintain edge information and not produce any new artificial pixel intensity. The

proposed system uses the proposed picture quality improvement technique to distinguish between normal and breast cancer cells. The segmentation mechanism will be discussed in the following section.

Segmentation

If the image is not accurately segmented, additional structures besides nuclei, such as cytoplasm and stoma, will be present alongside the seats which can result in overlapping hearts or the heterogeneous nature of breast tissue, which can eventually taint the image and increase the risk of an erroneous classification option being made because it has been proven effective for categorizing round-shaped objects (Sánchez-Cauce *et al*., 2021; Jarosik *et al*., 2020). To do an automated analysis of mammography images and detect breast cancer in its early stages, one of the essential steps is segmenting the Region of Interest (RoI). Each pixel in the dataset imageries needs to be classified as either Background (BG) or the ROI (breast area) for the segmentation to be a classification problem. The mammography images are the phase's input and the ROI (breast regions) images are the phase's output. Both are combined with the original mammography images to produce the ROI images as input for the classifier phase.

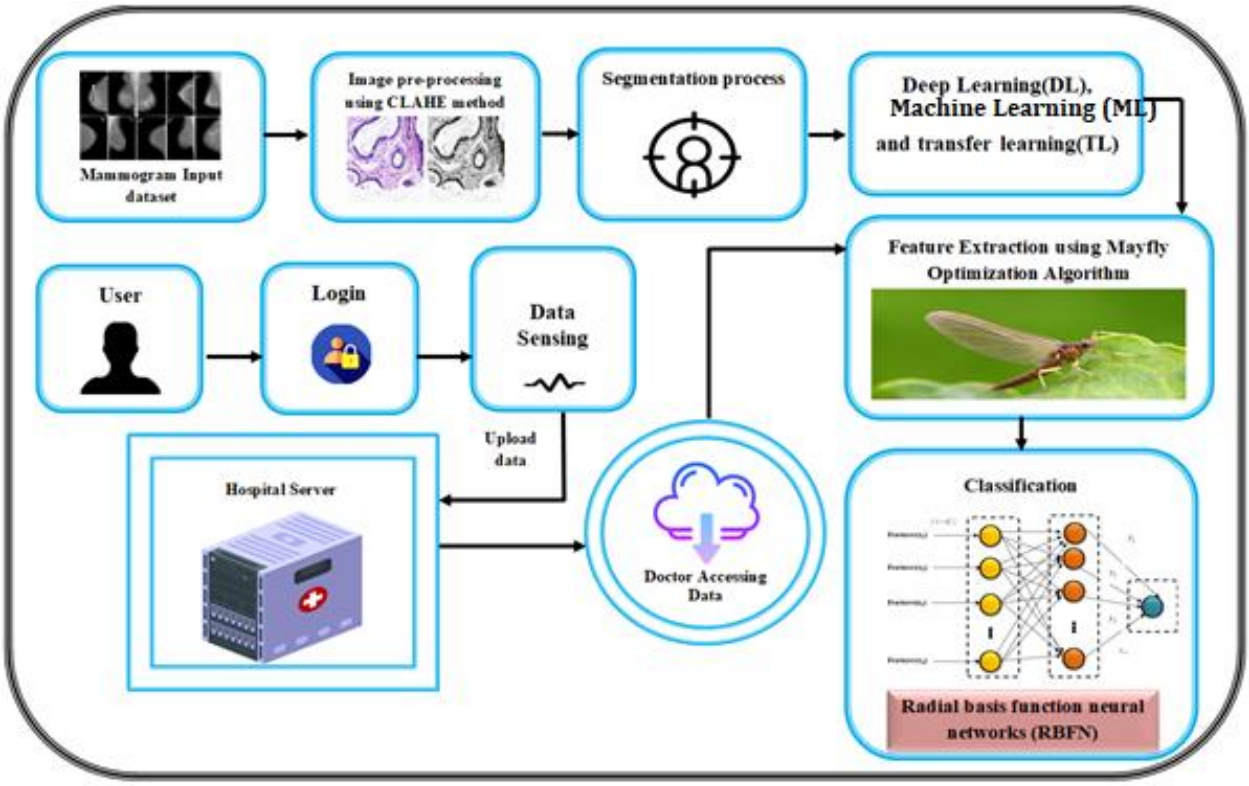

Fig. 1: Block diagram of RBFN-MOA proposed method

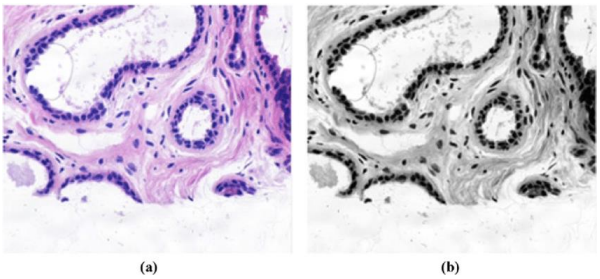

Fig. 2: (a) Histogram equalization before Pre-processing (b) Histogram equalization After Pre-processing

The proposed segmentation of the mammography pictures is done using the modified U-Net (U-shaped encoder-decoder network architecture) model. Encoder and decoder networks make up the modified U-Net segmentation. CNN's "encoder component" contains more semantic data than spatial data. Spatial information can be used to partition semantic data. U-Net receives technical data from the decoder component and semantic data from the network's lowest layer. Delicate segment structures are given through the exchange of high-resolution features from the encoder to the decoder without a connection. The patch size is 32 × 32 pixels and the highest layer uses 42 feature maps.

Feature Extraction Using the Mayfly Optimization Algorithm

The proposed method incorporates the firefly algorithm and Particle Swarm Optimization (PSO). The Mayfly Optimization Algorithm is a highly efficient hybrid optimization method that simulates mayfly mating behavior. This is illustrated in Fig. 3 which shows the working of MAO Algorithm. Particle swarm optimization, or PSO, improves its global search. Assuming that the mayfly matures into an adult soon after hatching and that only the healthiest individuals of the group survive, this optimization technique disregards the mayfly's lifespan. Each mayfly's location within the solution region indicates the possibility that a helpful solution will be located.

The presence of male or female mayflies is determined at random. To put it another way, the mayflies, the search agent, choose their beginning points at random inside the search space, *T* that is represented by the position vector of the mayflies $S=\left[s_1, s_2, ..., s_{d_{Max}}\right]^T$. The Objective Function (OF), symbolized by the *f*(*x*), is used to evaluate the performance of the position vector (*x*). Consider the velocity vector as an example $L=\left[l_1, l_2 ...., ld_{\max}\right]^T$, social and individual movement experiences determine the mayfly's new movement path in this technique, which is utilized to update position. As shown by and, the search agents alter their location to reflect their own best place and the work accomplished by other mayflies in the swarm. The first step of the MAO will be discussed in the following paragraphs.

Male Mayfly Flight

Male mayflies assemble in swarms, showing that their position shifts over time as a result of group and individual interactions. The correct positioning of a male mayfly is as surveys which can be calculated using the Eq. (1) as follows:

$$S_m(t+1)=l_m(t+1)+s_m(t) \tag{1}$$

Where, $s_m(t)$ is where the i^{th} mayfly is right now, assuming one exists and $s_m(0)$ the range of x_{Min} and x_{Max}. $s_m(t+1)$ and $l_m(t+1)$ are the mayfly's current positions and motion speed in the next time step.

The algorithm always assigns the same speed to male mayflies since they continue their courtship ritual at a height of a few meters, which may be discovered by doing the following steps:

$$\begin{aligned} l_{md}(t+1)=v_{md}(t)+q_1\times\exp(-\varsigma D_p^2)\times(sbest_{md}-s_{md}(t))+\\ q_2\times\exp(-\varsigma D_g^2)\times(gbest_d-s_{md}(t)) \end{aligned} \tag{2}$$

Here, q_1 and q_2 are positive attraction constants that individual interactions. A male mayfly's correct placement is as follows: D_p and D_p are the distances between *pi* $sbest_m$ and *gbest*, which are identified when Eqs. (4-5) are applied to the data l_{md} and s_{md} are, respectively, the i^{th} agent's speed and position in the d^{th} dimension where d = 1, 2, 3, . . ., d_{Max}. $sbest_{md}$ reflects the highest level of achievement obtained by the i^{th} agent of the d^{th} dimension, which may be found by performing the following:

$$sbest_m=\begin{cases} x_m(t+1), & f(x_m(t+1))<f(sbest_m) \\ sbest_m, & f(x_m(t+1))\geq f(sbest_m) \end{cases} \tag{3}$$

Here, f (.) is the quality of the solution influenced by the OF. D_p^2 and D_g^2 according to the following Eqs. (4-5):

$$D_s^2=\left(\sum_{n=1}^{d_{Max}}\left(s_{md}-sbest_m\right)\right)^{0.5} \tag{4}$$

$$D_g^2=\left(\sum_{d=1}^{d_{Max}}\left(s_{md}-gbest\right)\right)^{0.5} \tag{5}$$

The mayflies with the highest fitness levels will begin the nuptial dance by performing vertical movements, ensuring that the algorithm continues to generate the best results. As a result, the most effective mayflies must maintain their speed change in the manner stated below, adding a random component to the algorithm as mentioned in Eq. (6):

$$l_{md}(t+1)=l_{md}(t)+ND\times\varpi \tag{6}$$

Here, in Nuptial Dance (ND) the symbol *ND* stands for the nuptial dance coefficient, which is a random value between -1 and 1.

Female Mayfly Flight

Female mayflies approach male mayflies rather than flying in swarms like their male counterparts when it's time to mate. The i^{th} female mayfly's position in the search space is represented as $r_m(t)$ and it can be updated utilizing the Eq. (7):

$$r_m(t+1)=l_m(t+1)+r_m(t) \tag{7}$$

According to attraction modeling, it is a deterministic process in which the fittest woman is drawn to the most appropriate male, and so on. Velocity can be calculated using the following Eq. (8):

$$l_{md}(t+1)=\begin{cases} l_{md}(t)+q_2\times\exp(-\varsigma D_{if}^2)\times(s_{md}(t)-r_{md}(t)), \\ \qquad f(r_m)>f(s_m) \\ u_{md}(t)+q_w\times\varpi, \quad f(r_m)\le f(p_m) \end{cases} \tag{8}$$

Here, $r_{md}(t)$ and $u_{md}(t)$ is the location and speed of the i^{th} female mayfly in the d^{th} dimension at time t. D_{if}^2 are the male-female distances in mayflies proportional to the square of two, q_w is a coefficient that is applied to a randomly chosen walk.

Mating Procedure

The crossover operator was used to mimic mayfly mating behavior, which is explained in greater detail in the following paragraphs. Just as males are drawn to females, one male and one female are picked from their respective sets to be the offspring's parents. The selection strategy could be random or based on the objective function mayflies in each group mate with opposing group members. For example, the fittest female will mate with the most suitable male, and so forth. The offspring of the crossover can be computed using the following Eqs. (9-10):

$$\vartheta 1=\gamma\times male+(1-\gamma)\times female \tag{9}$$

$$\vartheta 2=\gamma\times female+(1-\gamma)\times male \tag{10}$$

Here, $\vartheta 1$ and $\vartheta 2$ offspring 1 and 2, in that order. γ is a numeric value chosen randomly from each range? The terms male and female are frequently used to refer to the parents. It's important to note that an offspring's beginning speed is always zero miles per hour.

Algorithm 1: Pseudocode for Mayfly Optimization Algorithm

Objective function $f(x), x=(x_1,.....,x_d)^T$
Initialize the male mayfly population $S=\left[s_1,s_2,....,s_{d_{Max}}\right]^T$ and velocities
Initialize the female mayfly population $R=\left[r_1,r_2,....,r_{d_{Max}}\right]^T$ andvelocities
Evaluate solutions
Find global best gbest
Do While stopping criteria are not met
    Update velocities and solutions of males and females
    Evaluate solutions
    Rank the mayflies
    Mate the mayflies
    Evaluate offspring
    Separate offspring to male and female randomly
    Replace the worst solutions with the best new ones
    Update sbest and gbest
End While
Post-process results and visualization

In the proposed work the equations were changed in order to describe how individuals in mayfly swarms evolve to improve the MAO technique. Every simulation analysis revealed that the enhanced MAO algorithm would outperform the baseline method. First started to discover that certain non-symmetric benchmark functions can be efficiently optimized. The simulation results for the non-symmetric benchmark functions employed in this study revealed that the MAO approach and its upgrades could not improve any non-symmetric benchmark functions.

Initialize the male mayfly population $S=\left[s_1,s_2,....,s_{d_{Max}}\right]^T$ and velocities then Initialize the female mayfly population $R=\left[r_1,r_2,....,r_{d_{Max}}\right]^T$ and velocities. Evaluate solutions, rank the mayflies, Mate the mayflies, Update velocities and solutions of males and females, evaluate offspring, Separate offspring to male and female randomly, replace worst solutions with the best new ones, and finally update sbestandgbest. Repeat the process until the stopping criteria are not met. Find the global best gbest as a result and visualize at the end.

Classification Using Radial Basis Function Neural Networks (RBFN)

A Radial Basis Function (RBF) network is a three-layer feed-forward neural network in its most basic form. The first layer houses the contributions to the network. One or more RBF non-linear activating units make up the second layer, a buried layer. The top layer represents the output of the network. Gaussian functions are widely used to construct RBFN activation functions. Figure 4 depicts the RBFN structure. Assume a data set named *D* and *N* patterns of the form (*xp*, *yp*), where *xp* represents the data set's input and *yp* represents its actual output.

Applying Eq. (11), you could determine the hidden layers with the activation function's output varies according to how far the input pattern *x* is from the network's center:

$$\phi_i(\|x-d_i\|)=exp\left(-\frac{\|x-d_i\|^2}{2\sigma^2{}_j}\right) \tag{11}$$

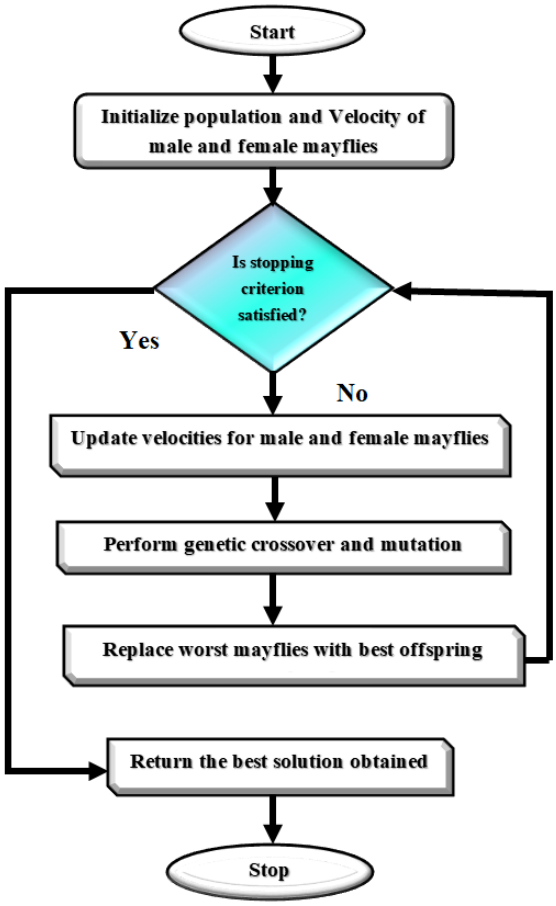

Fig. 3: Flowchart of MAO algorithm

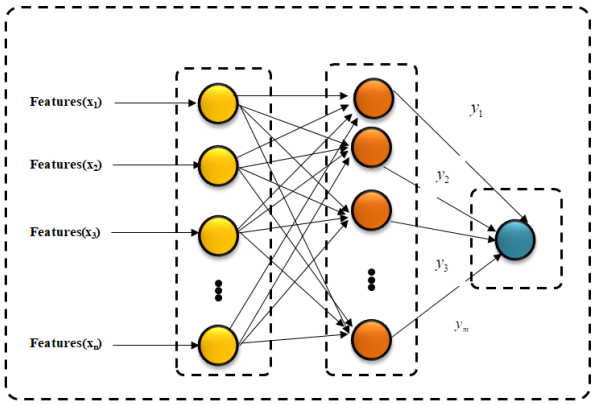

Fig. 4: Structure of RBFN

Here, ||.|| is the Euclidean norm and in this case, and are, respectively, the center and breadth of the hidden neuron *j*.

The output of node *k* on the network's output layer can then be considered using the calculation mentioned in Eq. (12):

$$yk = \sum_{j=1}^{n} \omega jk\phi_j(x) \tag{12}$$

Most of the traditional ways to train RBFNs described in the literature are done in two steps. In the first stage, an unsupervised clustering algorithm is used to find the centers and widths. The second stage of the approach is choosing the connection weights between the hidden layer and the output layer so that an error criterion, such as the Mean Squared Error (MSE), is minimized throughout the entire data set.

Implementation and Data Set Details

The proposed Python network model is run on a single NVIDIA Titan × Pascal GPU (12G) with an eight-batch size. The learning rates of criticism and classification networks will be flexibly decreased during Adam optimizer training. The learning rates of these two types of networks are set at 5e-3 and 1e-3, respectively. As a trade-off between computation expense and accuracy, the discrimination network's K = 3 critics and it is ten balancing factors are both set.

Experiments for the proposed technique are carried out on the CBIS-DDSM database (Lee *et al*., 2017). This collection has 59322 breast images, each measuring 1024 by 1024 pixels. This Curated Breast Imaging Subset of DDSM (CBIS-DDSM) is an updated and standardized version of the Digital Database for Screening Mammography (DDSM). The DDSM is a database of 2,620 scanned film mammography studies. It contains normal, benign, and malignant cases with verified pathology information. The scale of the database along with ground truth validation makes the DDSM a useful tool in the development and testing of decision support systems.

Evaluation Metrics

The classification results are listed in the confusion matrix. The confusion matrix aids professionals in determining whether the results are high-quality. Inaccurate negative projections are the most dangerous in the medical industry. Several performance measures were produced using a confusion matrix. The accuracy was calculated based on examples with appropriate identification. The method for computing precision is provided by Eq. (13):

$$Accuracy = \frac{TP+TN}{TP+FN+FP+TN} \tag{13}$$

Precision: Calculated by comparing the proportion of genuine positive pixels to the sum of actual positive pixels and fake positive pixels using Eq. (14):

$$Precision = \frac{TP}{TP + FP} \tag{14}$$

Recall: Recall is computed using Eq. 15 and the ratio of the entire amount of valid positive pixels to the entire amount of actual positive pixels plus the total number of false negative pixels is determined by Eq. (15):

$$Recall = \frac{TP}{TP + FN} \tag{15}$$

F1-Score: F1-Score, which represents how well the system functions overall, is calculated using Eq. (16):

$$F1 - Score = 2 * \frac{Precision * \mathrm{Re}call}{Precision + \mathrm{Re}call} \tag{16}$$

TP stands for accurately detected true-positive pixels. *FP* False-Positive Pixels (FP) occur when pixels that aren't part of the breast cancer images are improperly identified as such. In contrast, False-Negative pixels (FN) happen when the backdrop is incorrectly identified as such.

The metric Root Mean Squared Error (RMSE) is defined as:

$$RMSE = \sqrt{\frac{1}{T}\sum_{I,J}\left(R_{ij} - R_{ij}\right)^2} \tag{17}$$

Results and Discussion

Experiments for the proposed technique are carried out on the CBIS-DDSM database (Lee *et al*., 2017). The mammography was initially with a Contrast-Limited Adaptive Histogram Equalization (CLAHE) filter utilized during pre-processing before being sent to the next stage. CLAHE filter was designed to pre-process the noisy material in the MRI picture. The Connected Component Labelling method can determine the largest breast region. The database and the breast image details are mentioned in the Fig. 5. The breast is the only piece after removing the minor, undesirable component of the binary image. The binary mask that remains in the breast region is then retrieved from the mammogram using a noise-reduced mammography that multiplies the show, one element at a time, with the cover. Reduce the size of the image to speed up the calculation. The smaller the picture, then the faster the extraction method. Before being saved, the idea is cropped to make it smaller. After pre-processing, the breast ROI region is extracted from the image using the segmentation process. During the feature extraction stage, the first-order statistical feature and second-order are determined by MOA textural components. Convolution Neural Network-You only Look Once (CNN-YOLO), Residual Networks (ResNet50), Diffusion Convolution Neural Network (DCNN), Visual Geometry Group (VGG16), Support Vector Machine (SVM), and Convolution Neural Network (CNN) were among the techniques compared in this study.

Discussion on Models Used

ResNet-50 is a 50-layer convolution neural network (48 convolution layers, one MaxPool layer, and one average pool layer). Residual neural networks are a type of Artificial Neural Network (ANN) that forms networks by stacking residual blocks. The 50-layer ResNet uses a bottleneck design for the building block. A bottleneck residual block uses 1×1 convolutions, known as a "bottleneck", which reduces the number of parameters and matrix multiplications. This enables much faster training of each layer. It uses a stack of three layers rather than two layers.

YOLO makes use of only convolution layers, making it a Fully Convolution Network (FCN). It has:

- 75 convolution layers with skip connections and up-sampling layers
- No form of pooling is used
- a convolution layer with stride 2 is used to down sample the feature maps. This helps in preventing the loss of low-level features often attributed to pooling

Being a Fully Convolution Network (FCN), YOLO is invariant to the size of the input image. A big one of these problems is that if we want to process our images in batches (images in batches can be processed in parallel by the Graphical Processing Unit (GPU), leading to speed boosts), which need to have all images of fixed height and width. This process is needed to concatenate multiple images into a large batch. The network down samples the image by a factor called the stride of the network.

CNN is a mathematical construct that is typically composed of three types of layers (or building blocks): Convolution, pooling, and fully connected layers. The first two, convolution and pooling layers, perform feature extraction, whereas the third, a fully connected layer, maps the extracted features into the final output, such as classification. A convolution layer plays a key role in CNN, which is composed of a stack of mathematical operations, such as convolution, a specialized type of linear operation.

Support Vector Machine (SVM) works in a similar fashion to linear discriminant analysis. A hyperplane or

set of hyperplanes is created, in order to separate the feature vectors into several classes like Linear Discriminant Analysis (LDA), but it selects the hyperplane which is at maximum distance from the nearest training samples. SVM finds the hyperplane with the maximal margin according to cover's theorem by mapping input data into high-dimensional space.

Discussion on the Result of Pre-Processing

Improved comprehension is ensured using image-enhancing techniques. Histogram equalization is one method of increasing the dynamic range of the pixel intensity distribution. Breast cancer image histograms based on contrast which is narrow and focused exclusively on particular grey level values show that which often have shallow contrast. In contrast, the reduced difference in breast cancer pictures obscures the fine details of the lesions, making them challenging to present to specialists. There is a risk of incorrect therapy as a result of this delay. Such situations necessitate histogram equalization, which ignores local variations entirely.

Because of the higher background in homogeneities produced by the CLAHE algorithm, some post-processing is necessary for medical imaging. Image quality can be improved by employing a CLAHE-based technique, which is detailed in this article. This is illustrated in Fig. 6 (a-b) by a succession of non-overlapping "tiles" that the algorithm creates from the image.

Discussion on the Result of Segmentation

To do an automated analysis of mammography images and detect breast cancer in its early stages, one of the essential steps is segmenting the Region of Interest (RoI). This is illustrated in Fig. 7 (a-b) as each pixel in the dataset imageries needs to be classified as either Back Ground (BG) or the ROI (breast area) for the segmentation to be a classification problem. The mammography images are the phase's input and the ROI (breast regions) images are the phase's output. Both are combined with the original mammography images to produce the ROI images as input for the classifier phase. Our segmentation of the mammography pictures is done using the modified U-Net model. CNN's "encoder component" contains more semantic data than spatial data. Spatial information can be used to partition semantic data. U-Net receives technical data from the decoder component and semantic data from the network's lowest layer. Delicate segment structures are given through the exchange of high-resolution features from the encoder to the decoder without a connection. The patch size is 32 ×32 pixels and the highest layer uses 42 feature maps.

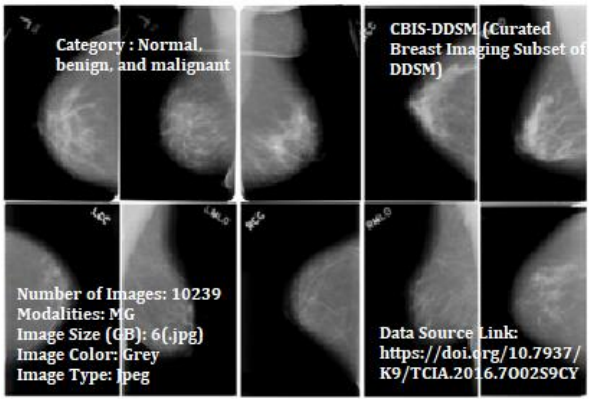

Fig. 5: Breast cancer image dataset

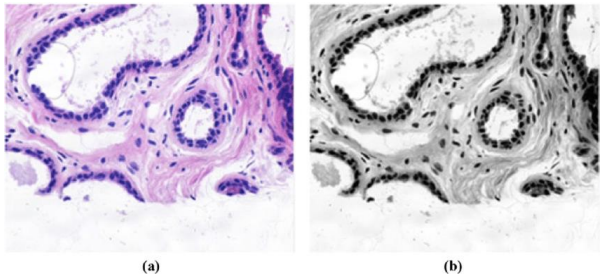

Fig. 6: (a) Before pre-processing (b) After pre-processing

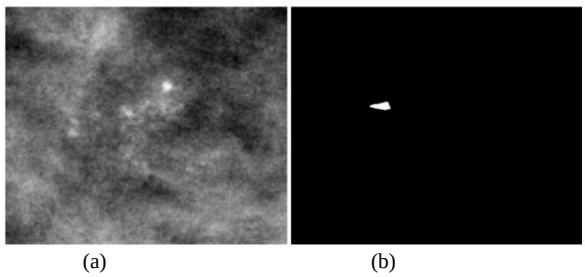

Fig. 7: (a) Before segmentation (b) After segmentation

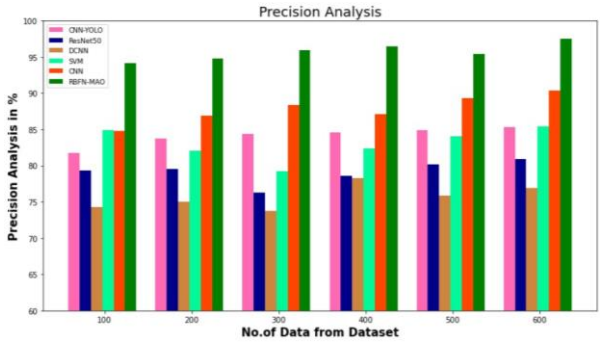

Fig. 8: Precision analysis for RBFN-MOA method with existing systems

Discussion on Result Analysis of Evaluation Metrics

Precision

A comparison of the precision of the RBFN-MAO approach and other existing techniques is shown in Fig. 8 and Table. 2. The graph demonstrates how the deep learning strategy has improved performance and precision. For instance, the RBFN-MAO model has a precision value of 94.16% for data size 100, compared to precision values of 81.75, 79.27, 74.327, 84.93, and 84.83% for the CNN-YOLO, ResNet50, DCNN, SVM, and CNN models. The RBFN-MAO model has demonstrated its best performance with various data sizes. Similarly, under 600 data points, RBFN-precision MAO's value is 97.54%, whereas, for CNN-YOLO, ResNet50, DCNN, SVM, and CNN models, it is 85.28, 80.95, 76.94, 85.39 and 90.32%, respectively.

Recall

A comparison of the RBFN-MAO strategy with various known techniques is shown in Fig. 9 and Table. 3. The chart demonstrates that the deep learning approach has led to improved recall performance. For instance, with data size 100, the recall value for the RBFN-MAO model is 94.28%, compared to recall discounts of 85.90, 74.59, 92.45, 78.49, and 82.17% for the CNN-YOLO, ResNet50, DCNN, SVM, and CNN models. The RBFN-MAO model has demonstrated its best performance with various data sizes. The recall value of the RBFN-MAO is 97.51% under 600 data points, whereas it is 88.36, 76.38, 94.54, 80.36, and 85.73% for the CNN-YOLO, ResNet50, DCNN, SVM, and CNN models, respectively.

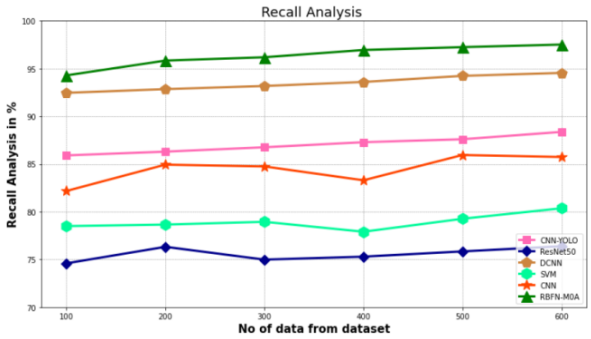

Fig. 9: Recall Analysis for RBFN-MOA method with existing systems

Table 2: Precision analysis for the RBFN-MOA approach using existing systems

No data from dataset	CNN-YOLO	ResNet50	DCNN	SVM	CNN	RBFN-MAO
100	81.75	79.27	74.32	84.93	84.83	94.16
200	83.76	79.56	75.06	82.09	86.90	94.78
300	84.37	76.31	73.75	79.23	88.32	95.93
400	84.55	78.54	78.29	82.39	87.05	96.41
500	84.90	80.13	75.83	84.07	89.27	95.39
600	85.28	80.95	76.94	85.39	90.32	97.54

Table 3: Recall Analysis for RBFN-MOA method with existing systems

No data from dataset	CNN-YOLO	ResNet50	DCNN	SVM	CNN	RBFN-MAO
100	85.90	74.59	92.45	78.49	82.17	94.28
200	86.29	76.32	92.84	78.65	84.93	95.83
300	86.75	74.98	93.17	78.94	84.74	96.18
400	87.28	75.29	93.59	77.90	83.29	96.94
500	87.59	75.84	94.23	79.26	85.94	97.24
600	88.36	76.38	94.54	80.36	85.73	97.51

Table 4: F-score Analysis for RBFN-MOA method with existing systems

No data from dataset	CNN-YOLO	ResNet50	DCNN	SVM	CNN	RBFN-MAO
100	69.57	87.43	78.37	73.90	83.29	93.04
200	70.54	87.94	76.35	75.37	85.17	95.84
300	74.73	88.21	77.92	74.04	84.05	94.97
400	73.19	88.73	78.48	76.28	86.50	95.10
500	75.28	89.75	78.85	79.43	89.35	96.39
600	75.83	90.64	82.10	80.02	92.45	97.48

Table 5: Accuracy Analysis of RBFN-MOA Method with existing systems

No data from dataset	CNN-YOLO	ResNet50	DCNN	SVM	CNN	RBFN-MAO
100	78.56	86.17	73.90	82.03	87.39	93.87
200	79.49	85.29	75.82	81.95	87.94	94.13
300	80.54	85.46	74.37	82.74	88.58	95.38
400	81.27	86.27	74.69	83.29	89.37	96.59
500	82.38	87.39	76.29	84.59	90.73	96.97
600	83.74	88.73	77.38	85.74	91.36	97.16

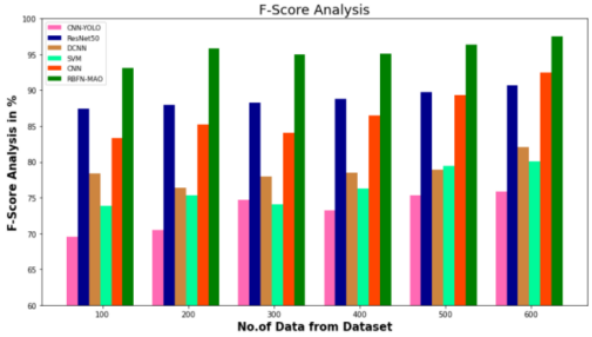

Fig. 10: F-Score Analysis for RBFN-MOA method with existing systems

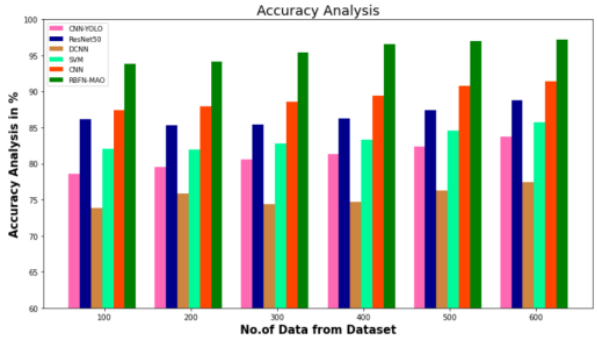

Fig. 11: Accuracy analysis of RBFN-MOA method with existing systems

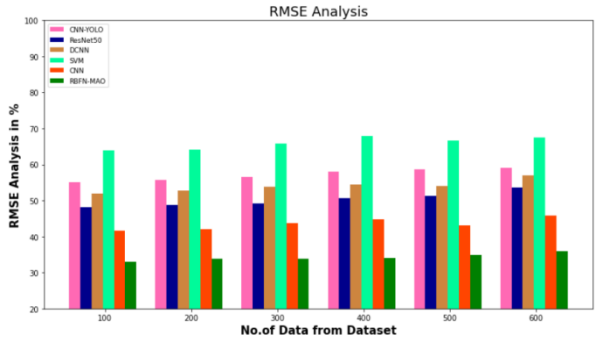

Fig. 12: RMSE for RBFN-MOA method with existing systems

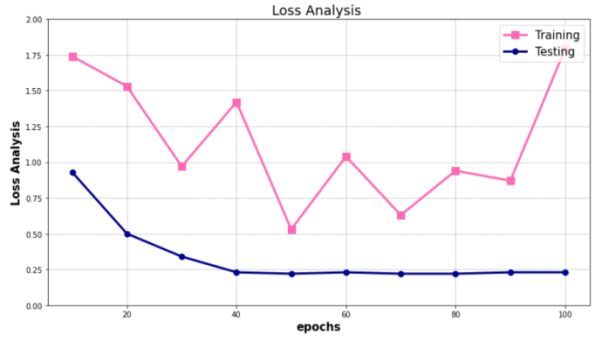

Fig. 13: Loss Analysis for RBFN-MOA method

F-Score

Figure 10 and Table 4 depict an F-Score comparison of the RBFN-MAO strategy with other known methodologies. The figure demonstrates how the deep learning approach improved F-Score performance. For instance, the RBFN-MAO model has an F-Score of 93.04% with data size 100, whereas the CNN-YOLO, ResNet50, DCNN, SVM, and CNN models have F-Scores of 69.57, 87.43, 78.37, 73.90 and 83.29%, correspondingly. However, the RBFN-MAO model performed best with various data sizes. Similarly, under 600 data points, the F-Score value of RBFN-MAO is 97.48, 75.83, 90.64, 82.10, 80.02, and 92.45% for CNN-YOLO, ResNet50, DCNN, SVM, and CNN models, respectively.

Accuracy

A comparison of the accuracy of the RBFN-MAO approach and other existing techniques is shown in Fig. 11 and Table. 5. The graph demonstrates that the deep learning strategy has improved performance and accuracy. For instance, with data size 100, the accuracy value for RBFN-MAO is 93.87%, whereas the accuracy values for CNN-YOLO, ResNet50, DCNN, SVM, and CNN models are, respectively, 78.56, 86.17, 73.90, 82.03 and 87.39%. The RBFN-MAO model has demonstrated its best performance with various data sizes. Like this, under 600 data points, RBFN-accuracy MAO's value is 97.16%, whereas, for CNN-YOLO, ResNet50, DCNN, SVM, and CNN models, it is 83.74, 88.73, 77.38, 85.74 and 91.36%, respectively.

RMSE

Table 6 and Fig. 12 explain the RMSE analysis of the RBFN-MAO method with other existing techniques. For example, with 100 data points, the suggested technique has an RMSE of 32.895%, whereas CNN-YOLO, ResNet50, DCNN, SVM, and CNN have RMSEs of 55.067, 48.076, 52.007, 63.857and 41.539%, respectively. The RBFN-MAO approach performs better and has a lower RMSE. Similarly, the suggested technique has an RMSE of 35.856% with 600 data points, whereas the methods for CNN-YOLO, ResNet50, DCNN, SVM, and CNN have RMSEs of 59.146, 53.674, 56.905, 67.549, and 45.764%, respectively.

Loss Analysis

Figure 13 and Table 7 demonstrate the outcomes of the loss analysis done on the training and testing datasets using the RBFN-MAO technique. The figure indicates a loss of 1.74 after ten training rounds and a loss of 0.93 after ten testing and validation rounds. Following 90 epochs, the validation loss for testing is 0.23 and the failure for training is 0.87. Statistics show that the proposed strategy has the lowest loss compared to other approaches over various epochs.

Table 6: RMSE for RBFN-MOA method with existing systems

No data from dataset	CNN-YOLO	ResNet50	DCNN	SVM	CNN	RBFN-MAO
100	55.067	48.076	52.007	63.857	41.539	32.895
200	55.798	48.798	52.673	64.036	42.070	33.784
300	56.498	49.285	53.895	65.783	43.673	33.905
400	57.985	50.645	54.509	67.921	44.854	34.127
500	58.653	51.342	54.067	66.541	43.037	34.796
600	59.146	53.674	56.905	67.549	45.764	35.856

Table 7: Loss Analysis for RBFN-MOA method

Epochs	Training validation	Testing validation
10	1.74	0.93
20	1.53	0.50
30	0.97	0.34
40	1.42	0.23
50	0.53	0.22
60	1.04	0.23
70	0.63	0.22
80	0.94	0.22
90	0.87	0.23
100	1.79	0.23

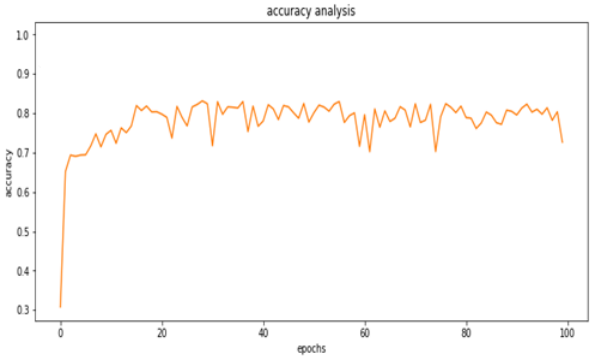

Fig. 14: Accuracy analysis graph with no. of epochs

Accuracy Analysis with Epochs

Figure 14, the accuracy of the proposed method is evaluated with no. of epochs. The graph shows that the performance and accuracy of the proposed method have increased. In contrast to accuracy values of 80.98, 87.33, 84.22, 82.89, and 85.19% for 20,40,60,80 and 100 epochs, respectively. The RBFN-MAO model, however, has demonstrated its best performance with various epochs.

Conclusion

Patients receiving breast cancer diagnosis and treatment as soon as possible have a better chance of surviving and recovering. Using breast MRI data and the Mayfly Optimization Algorithm, the authors of this study developed a new Radial Basis Function Networks (RBFN) model to identify breast cancer at an earlier stage (MAO). The system is trained on breast MRI data before employing a cutting-edge CLAHE filter to pre-process the noisy MRI image data. After the background was removed from breast cancer images, a CLAHE filter was used to finish the image restoration procedure. A Python simulation of this model is also run and the findings are compared to the ongoing research. Compared to earlier models, the proposed RBFN-MAO model provides the best performance and precision. The accuracy of the recommended model is 98.435%, whereas the CNN technique, SVM, DCNN, ResNet50, and CNN-YOLO have accuracy ratings of 87.826, 92.547, 89.453, 84.754, and 95.546%, respectively. Future performance will be improved by resisting adversarial assaults and reducing design time by combining hybrid optimization with a security measure for modifying design parameters. As a result, less design time will be needed.

Acknowledgment

We are extremely grateful to "Sathyabama University" and the study's Research Supervisor, Dr. R. Aroul Canessane, for their steadfast assistance and extended support in distributing this research report.

Funding Information

The authors have not received any financial support or funding to report.

Author's Contributions

Anitha Ponraj: Conception a design of the article and studied previous research, working on graphs, delving into the results of algorithms, analyzed them, and extracted the final results, equations, and tables of results. She studied previous research and suggested a new contribution.

Aroul Canessane: He supervised the work done in this study and drafted the paper in terms of technical and English proofreading for important intellectual content.

Ethics

The corresponding author confirms and attests that other authors reviewed and approved the work and that there were no ethical dilemmas. The reference section included complete and accurate citations for each source.

References

Baffa, M. D. F. O., & Lattari, L. G. (2018, October). Convolutional neural networks for static and dynamic breast infrared imaging classification. In 2018 31st Sibgrapi Conference on Graphics, Patterns and Images (SIBGRAPI), (pp. 174-181). IEEE. https://doi.org/10.1109/SIBGRAPI.2018.00029

Brennan, P. C., Gandomkar, Z., Ekpo, E. U., Tapia, K., Trieu, P. D., Lewis, S. J., ... & Evans, K. K. (2018). Radiologists can detect the 'gist'of breast cancer before any overt signs of cancer appear. *Scientific Reports*, *8*(1), 1-12. https://doi.org/10.1038/s41598-018-26100-5

Charan, S., Khan, M. J., & Khurshid, K. (2018, March). Breast cancer detection in mammograms using convolutional neural network. In *2018 International Conference on Computing, Mathematics and Engineering Technologies (iCoMET)*, (pp. 1-5). IEEE. https://doi.org/10.1109/ICOMET.2018.8346384

Chiang, T. C., Huang, Y. S., Chen, R. T., Huang, C. S., & Chang, R. F. (2018). Tumor detection in automated breast ultrasound using 3-D CNN and prioritized candidate aggregation. *IEEE Transactions on Medical Imaging*, *38*(1), 240-249. https://doi.org/10.1109/TMI.2018.2860257

Chouhan, N., Khan, A., Shah, J. Z., Hussnain, M., & Khan, M. W. (2021). Deep convolutional neural network and emotional learning based breast cancer detection using digital mammography. *Computers in Biology and Medicine*, *132*, 104318. https://doi.org/10.1016/j.compbiomed.2021.104318

Duffy, S. W., Tabár, L., Yen, A. M. F., Dean, P. B., Smith, R. A., Jonsson, H., ... & Chen, T. H. H. (2020). Mammography screening reduces rates of advanced and fatal breast cancers: Results in 549,091 women. *Cancer*, *126*(13), 2971-2979. https://doi.org/10.1002/cncr.32859

Ellmann, S., Seyler, L., Evers, J., Heinen, H., Bozec, A., Prante, O., ... & Baeuerle, T. (2019). Prediction of early metastatic disease in experimental breast cancer bone metastasis by combining PET/CT and MRI parameters to a Model-Averaged Neural Network. Bone, 120, 254-261. https://doi.org/10.1016/j.bone.2018.11.008

Gaikwad, V., J. (2015). Detection of breast cancer in mammogram using support vector machine. *International Journal of Scientific Engineering and Research (IJSER).10*(1):19-21. https://scholar.google.com/citations?view_op=view_citation&hl=en&user=3UxOrvcAAAAJ&citation_for_view=3UxOrvcAAAAJ:u-x6o8ySG0sC

Gbenga, D. E., Christopher, N., Yetunde, D. C., & Maiduguri, N. (2017). Performance comparison of machine learning techniques for breast cancer detection. *Nova*, *6*(1), 1-8. https:// doi.org/10.20286/nova-jeas-060105

George, K., & Sankaran, P. (2020). Computer assisted recognition of breast cancer in biopsy images via fusion of nucleus-guided deep convolutional features. *Computer Methods and Programs in Biomedicine*, *194*, 105531. https://doi.org/10.1016/j.cmpb.2020.105531

Guan, S., Kamona, N., & Loew, M. (2018, October). Segmentation of thermal breast images using convolutional and deconvolutional neural networks. In *2018 IEEE Applied Imagery Pattern Recognition Workshop (AIPR)*, (pp. 1-7). IEEE. https://doi.org/10.1109/AIPR.2018.8707379

Houssami, N., Lee, C. I., Buist, D. S., & Tao, D. (2017). Artificial intelligence for breast cancer screening: Opportunity or hype?. *The Breast*, *36*, 31-33. https://doi.org/10.1016/j.breast.2017.09.003

Huang, M. W., Chen, C. W., Lin, W. C., Ke, S. W., & Tsai, C. F. (2017). SVM and SVM ensembles in breast cancer prediction. *PloS One*, *12*(1), e0161501. https://doi.org/10.1371/journal.pone.0161501

Iqbal, H. T., Majeed, B., Khan, U., & Altaf, M. A. B. (2019, October). An infrared high classification accuracy hand-held machine learning based breast-cancer detection system. In *2019 IEEE Biomedical Circuits and Systems Conference (BioCAS)*, (pp. 1-4). IEEE. https://doi.org/10.1109/BIOCAS.2019.8918687

Jarosik, P., Klimonda, Z., Lewandowski, M., & Byra, M. (2020). Breast lesion classification based on ultrasonic radio-frequency signals using convolutional neural networks. *Biocybernetics and Biomedical Engineering*, *40*(3), 977-986. https://doi.org/10.1016/j.bbe.2020.04.002

Kim, C. M., Park, R. C., & Hong, E. J. (2020). Breast mass classification using eLFA algorithm based on CRNN deep learning model. *IEEE Access*, *8*, 197312-197323. https://doi.org/10.1109/ACCESS.2020.3034914

Kooi, T., Litjens, G., Van Ginneken, B., Gubern-Mérida, A., Sánchez, C. I., Mann, R., ...& Karssemeijer, N. (2017). Large scale deep learning for computer aided detection of mammographic lesions. *Medical Image Analysis*, *35*, 303-312. https://doi.org/10.1016/j.media.2016.07.007

Le, H., Gupta, R., Hou, L., Abousamra, S., Fassler, D., Torre-Healy, L., …& Saltz, J. (2020). Utilizing automated breast cancer detection to identify spatial distributions of tumor-infiltrating lymphocytes in invasive breast cancer. *The American Journal of Pathology*, *190*(7), 1491-1504. https://doi.org/10.1016/j.ajpath.2020.03.012

Lee, R., S. Gimenez, F.Hoogi, A., Miyake K., K, Gorovoy M, & Rubin D., L. (2017). A curated mammography data set for use in computer-aided detection and diagnosis research. *Sci Data*. 2017 Dec 19;4:170177. https://doi.org/10.1038/sdata.2017.177

Mambou, S. J., Maresova, P., Krejcar, O., Selamat, A., & Kuca, K. (2018). Breast cancer detection using infrared thermal imaging and a deep learning model. *Sensors*, *18*(9), 2799. https://doi.org/10.3390/s18092799

Mohammed, F. E., Zghal, N. S., Aissa, D. B. & El-Gayar, M. M. (2022). Classify Breast Cancer Patients using Hybrid Data-Mining Techniques. *Journal of Computer Science*, *18*(4), 316-321. https://doi.org/10.3844/jcssp.2022.316.321

Motlagh, M. H., Jannesari, M., Aboulkheyr, H., Khosravi, P., Elemento, O., Totonchi, M., & Hajirasouliha, I. (2018). Breast cancer histopathological image classification: A deep learning approach. *BioRxiv*, 242818. https://doi.org/10.1101/242818

Oladipupo, O. O., Adubi, S., Oyelade, O. J., & Omogbadegun, Z. O. (2020). An interval type-2 fuzzy association rule mining approach to pattern discovery in breast cancer dataset. *Journal of Computer Science*, *17*(3), 330-348. https://doi.org/10.3844/jcssp.2021.330.348

Piantadosi, G., Sansone, M., Fusco, R., & Sansone, C. (2020). Multi-planar 3D breast segmentation in MRI via deep convolutional neural networks. Artificial Intelligence in Medicine, 103, 101781. https://doi.org/10.1016/j.artmed.2019.101781

Sadhukhan, S., Upadhyay, N., & Chakraborty, P. (2020). Breast cancer diagnosis using image processing and machine learning. In *Emerging Technology in Modelling and Graphics: Proceedings of IEM Graph 2018* (pp. 113-127). Springer Singapore. https://doi.org/10.1007/978-981-13-7403-6_12

Siegel, R.L., Miller, K.D. & Jemal, A. (2020), Cancer statistics, 2020. *CA A Cancer J Clin*, 70: 7-30. https://doi.org/10.3322/caac.21590

Sánchez-Cauce, R., Pérez-Martín, J., & Luque, M. (2021). Multi-input convolutional neural network for breast cancer detection using thermal images and clinical data. *Computer Methods and Programs in Biomedicine*, *204*, 106045. https://doi.org/10.1016/j.cmpb.2021.106045

Singh, R., Ahmed, T., Kumar, A., Singh, A. K., Pandey, A. K., & Singh, S. K. (2020). Imbalanced breast cancer classification using transfer learning. *IEEE/ACM Transactions on Computational Biology and Bioinformatics*, *18*(1), 83-93. https://doi.org/10.1109/TCBB.2020.2980831

Sung, H., Ferlay, J., Siegel, R. L., Laversanne, M., Soerjomataram, I., Jemal, A., & Bray, F. (2021). Global cancer statistics 2020: GLOBOCAN estimates of incidence and mortality worldwide for 36 cancers in 185 countries. *CA: A Cancer Journal for Clinicians*, *71*(3), 209-249. https://doi.org/10.3322/caac.21660

Svensson, B. J., Dylke, E. S., Ward, L. C., Black, D. A., & Kilbreath, S. L. (2020). Screening for breast cancer-related lymphoedema: Self-assessment of symptoms and signs. *Supportive Care in Cancer*, *28*, 3073-3080. https://doi.org/10.1007/s00520-019-05083-7

Wang, H., Zheng, B., Yoon, S. W., & Ko, H. S. (2018). A support vector machine-based ensemble algorithm for breast cancer diagnosis. *European Journal of Operational Research*, *267*(2), 687-699. https://doi.org/10.1016/j.ejor.2017.12.001

Warren Burhenne, L. J., Wood, S. A., D'Orsi, C. J., Feig, S. A., Kopans, D. B., O'Shaughnessy, K. F., ... &Castellino, R. A. (2000). Potential contribution of computer-aided detection to the sensitivity of screening mammography. *Radiology*, *215*(2), 554-562. https://doi.org/10.1148/radiology.215.2.r00ma15554

Woodard, D. B., Gelfand, A. E., Barlow, W. E., & Elmore, J. G. (2007). Performance assessment for radiologists interpreting screening mammography. *Statistics in Medicine*, *26*(7), 1532-1551. https://doi.org/10.1002/sim.2633

Xie, L., Zhang, L., Hu, T., Huang, H., & Yi, Z. (2020). Neural networks model based on an automated multi-scale method for mammogram classification. *Knowledge-Based Systems*, *208*, 106465. https://doi.org/10.1016/j.knosys.2020.106465

Zalloum, H. N., Al Zeer, S., Manassra, A., Abu Sara, M. R. & Alkhateeb, J. H. (2022). Breast Cancer Grading using Machine Learning Approach Algorithms. *Journal of Computer Science*, *18*(12), 1213-1218. https://doi.org/10.3844/jcssp.2022.1213.1218